Supplementary information

A High Performance All-Solid-State Lithium-Sulfur Battery with Lithium Thiophosphate Solid Electrolyte

Patrick Bonnick,[†1] Keita Niitani,[†1] Masafumi Nose,[2] Koji Suto,[1] Timothy S. Arthur[1] and John Muldoon*[1]

† - These authors contributed equally to this work.

1 - Toyota Research Institute of North America, 1555 Woodridge Ave, Ann Arbor, MI 48105, USA

2 - Advanced Material Engineering Div., Toyota Motor Corporation, 1200, Mishuku, Susono, Shizuoka, 410-1193, Japan

* Corresponding author e-mail: john.muldoon@toyota.com

Experimental Procedures

General atmosphere: To protect the electrolyte from air, all of the below procedures were conducted under an Ar gas atmosphere with < 0.1 ppm O_2 and H_2O, either inside a glove box or within sealed experimental vessels.

Synthesis of the solid electrolyte: amorphous Li_3PS_4·0.5LiI. In preparation, the ball-mill pot and ZrO_2 balls were dried overnight in a vacuum oven at 120°C. It is very important that all chemicals and hardware that contact the electrolyte are properly dried. Anhydrous LiI beads (Aldrich, 99.999%) were added to an agate mortar and ground by hand until pulverized. Then, 0.5419 g of LiI (4.05 mmol) was moved to a new mortar along with 0.5581 g of anhydrous Li_2S (12.15 mmol, Aldrich, 99.98%) and 0.8999 g of anhydrous P_2S_5 (4.05 mmol, Sigma-Aldrich, 99%) to form a mixture (2.0 g total) containing a molar ratio of Li_2S : P_2S_5 : LiI = 3 : 1 : 1. This mixture was ground by hand for 5 minutes and then transferred to a 45 mL ZrO_2 ball-mill pot along with 32 g of ZrO_2 balls (5 mm diameter). The lid and PTFE O-ring were replaced, then the pot was clamped within a steel vessel and ball-milled for 40 cycles using a planetary ball mill (Pulverisette 7, Fritsch). Each cycle consisted of spinning the pot for 1 h at 550 rpm and then resting the pot for 5 min. Afterward, the amorphous Li_3PS_4·0.5LiI powder was collected by dumping the ZrO_2 balls into a 425 μm-mesh

sieve and shaking it side-to-side. Some powder was also collected by scraping the walls of the pot with a steel spatula. Overall, 1.6 g of light-yellow powder was collected (an 80% yield). To form the highest conductivity, semi-crystalline phase, the amorphous Li_3PS_4·0.5LiI powder was annealed at 185°C for 3 h in a muffle furnace (Across International, CF1100) inside the glove box. The resulting powder was a lighter, greyish shade of yellow.

DSC analysis. Differential scanning calorimetry (DSC) analysis was carried out using a TA Instruments DSC 250. 5 mg of amorphous Li_3PS_4·0.5LiI was deposited into a hermetic, aluminum pan (TA Instruments) and sealed, within the Ar-filled glove box. Analysis was performed at scanning rate of 5 °C min^{-1} between 30 °C and 400 °C.

Powder XRD Analysis. A Rigaku SmartLab 3kW fitted with an Anton-Paar HTK 1200N oven chamber and capillary extension was used to collect the XRD patterns. The 0.5 mm diameter quartz capillary was filled with amorphous Li_3PS_4·0.5LiI and sealed with epoxy in the glove box before transferring it to the diffractometer. Patterns were collected with a 0.05° step size at a rate of 0.0378°/min from 10° to 60° (22 h run). After the amorphous material was scanned, the capillary was heated to a particular temperature for 3 h and then cooled back down to 25°C before performing another XRD scan. This was repeated for 110°C, 160°C, 185°, 195°C and 270°C in accordance with interesting positions on the DSC curve. The 185°C pattern was collected nine times to confirm that the pattern did not change with time and, therefore, that the sample was successfully protected from air. The repeated scans were then added together to form the final XRD pattern with a better signal-to-noise ratio than the single scans.

Raman Analysis. Raman spectroscopy was performed with a Horiba LabRAM HR spectrometer equipped with an inverted optical microscope. A 50x lwr objective lens was used to focus a 532 nm laser onto the powder sample, which was pressed against the inside surface of a sealed cuvette to protect it from air. The back-scattered light was dispersed using a 600 grating/mm grating onto a CCD camera. Spectra were collected by performing 20 sequential scans, each with a 1 second duration. Spectra were collected from four different spots on each sample and compared to confirm sample homogeneity.

SEM Analysis. SEM images were collected using a JEOL 7800 FLV at a magnification of 1000x with an acceleration voltage of 6 kV and a beam current of 8 (43 pA).

Conductivity measurement. 100 mg of Li_3PS_4·0.5LiI powder was added to the hole in a Macor ring (OD 3.0 cm diameter, ID 11.28 mm diameter, i.e. 1.0 cm^2) and cold-pressed between two steel pistons into a pellet under 6 tons of pressure for 5 min. Then, carbon-coated aluminum foil (MTI corp.) disks were placed against both sides of the pellet and the stack was pressed again under 3 tons for about 1 min. After removing the stack from the press, the pistons were anchored in place by a cell top and bottom, held together by insulated bolts. The bolts were tightened to 2 N·m, which provides a stack pressure of about 88 MPa. Finally, the cell was sealed in an argon-filled container and placed into a temperature-controlled oven. Electrochemical impedance spectroscopy was performed using a Bio-logic VMP3 potentiostat, with a frequency range from 100 Hz to 1 MHz and a potential amplitude of 100 mV. EIS was performed at temperatures from -10°C to 60°C in 10°C increments. The electrolyte resistance was determined from the EIS plots by extrapolating the low-frequency, linear section of the curves down to the x-axis, as described by Minami *et al*.[1]

Fabrication of Li/Li_3PS_4·0.5LiI/Li symmetric cells. 100 mg of Li_3PS_4·0.5LiI powder was added to the hole in a Macor ring (OD 3.0 cm diameter, ID 11.28 mm diameter, i.e. 1.0 cm^2) and cold-pressed between two steel pistons under 6 tons of pressure for 5 min to form a pellet. Separately, a thick Li disk (99.8%, Honjo Metal) was polished with a toothbrush, inserted into an LDPE bag and rolled to a final thickness of about 120 μm. 7/16-inch diameter disks were then punched from the flattened Li using a knife punch, which were then placed against both sides of the pellet as electrodes. Stainless-steel pistons (i.e. current collectors) were pressed against the Li on both sides of the pellet to form a stack, which was then sandwiched between cell top and bottom. Finally, insulated bolts were used to compress the cell to 29 MPa before placing the cell into an argon-filled container, which was then moved from the glove box to an oven for electrochemical testing.

Critical Current Density (CCD) test of Li/Li_3PS_4·0.5LiI/Li cells. Li metal was plated and stripped at step-wise-increased current densities using a Bio-logic VMP3 or VSP potentiostat. At 25°C, the

current density was increased in a stepwise manner from 0.1 mA/cm^2 to 1.0 mA/cm^2 in 0.1 mA/cm^2 steps. At 60°C, the current density was increased in a stepwise manner from 0.8 mA/cm^2 to 4.0 mA/cm^2 in 0.2 mA/cm^2 steps. Each current was applied using 1-hour half-cycles for 2 cycles. The CCD was ascribed to the current at which a sharp drop in potential was witnessed mid-half-cycle.

Galvanostatic cycling of Li/Li_3PS_4·0.5LiI/Li cells. Li metal was plated and stripped at a constant current density using a Bio-logic VSP potentiostat. Cycling was performed at 60°C, at 1 mA/cm^2 and with an areal capacity per half-cycle of 4 mAh/cm^2.

Fabrication of the composite, sulfur positive electrode. The electrode material was fabricated in a two-step process wherein the sulfur and conductive carbon were combined first to ensure good adhesion between the two before finally adding the solid electrolyte. First, 0.6481 g of sulfur powder (Aldrich, 99.98%) and 0.3519 g carbon nanofibers (CNF, Aldrich, 98%) were added to a mortar and hand-ground for 5 min. The mixture was then moved to a 45 mL of ZrO_2 pot with 32 g of ZrO_2 balls (5 mm diameter). The lid and PTFE O-ring were replaced, taped shut and then the pot was moved to the planetary ball-mill (Pulverisette 7, Fritsch) and run for 10 cycles. Each cycle consisted of spinning the pot for 1 h at 500 rpm and then resting the pot for 5 min. Afterward, the S/CNF composite was collected by dumping the ZrO_2 balls into a 425 μm-mesh sieve and shaking it side-to-side. Some powder was also collected by scraping the walls of the pot with a steel spatula. All the collected powder was hand-ground again in a mortar. Overall, 0.9 g of black powder was collected (a 90% yield). In the second step, 0.2700 g of S/CNF and 0.2300 g Li_3PS_4·0.5LiI were hand-ground together for 5 min to form a S : CNF : Li_3PS_4·½LiI composite with a weight ratio of 35 : 19 : 46. This composite was moved to the ball-mill pot and ball-milled again using the same conditions as above. About 0.4 g of composite was recovered (an 80% yield) and used to make sulfur, positive electrodes.

Fabrication of the S-composite/Li_3PS_4·0.5LiI/Li cells. 100 mg of Li_3PS_4·0.5LiI powder was added to the hole in a Macor ring (OD 3.0 cm diameter, ID 11.28 mm diameter, i.e. 1.0 cm^2) and cold-pressed between two steel pistons under 6 tons of pressure for 5 min to form a pellet. To make a positive electrode, 7.8 mg of the S-composite electrode powder (corresponding to a sulfur-loading

of 2.73 mg/cm^2 or 4.56 mAh/cm^2) was spread over one side of the pellet and pressed under 3 tons for 3 min. Separately, both sides of a thick Li disk (99.8%, Honjo Metal) were polished with a toothbrush before inserting the disk into an LDPE bag and rolling it to a final thickness of about 120 μm. A 7/16-inch diameter disk was then punched from the flattened Li using a knife punch and then placed against the other side of the pellet as the negative electrode. Stainless-steel pistons (i.e. current collectors) were pressed against both electrodes to form a stack, which was then sandwiched between the cell top and bottom. Finally, insulated bolts were used to compress the cell to 29 MPa before placing the cell into an argon-filled container, which was then moved from the glove box to an oven for electrochemical testing.

Galvanostatic cycling of S-composite/Li_3PS_4·0.5LiI/Li cells. The galvanostatic cycling experiment was carried out at 60°C using a Bio-logic VSP3 potentiostat. The cell was discharged at 2.28 mA/cm^2 (C/2), with a lower voltage limit of 1.5 V, and charged at 0.456 mA/cm^2 (C/10) with an upper voltage limit of 3.1 V. In this study, the coulombic efficiency was defined as the charge capacity divided by the preceding discharge capacity (Q_C/Q_D) because the sulfur active material begins in a charged state (i.e. empty of Li^+) and is the capacity-limited electrode. This way, the coulombic efficiency ideally represents the amount of Li^+ extracted from the positive electrode divided by the amount that was deposited into it.

Supplementary Figures

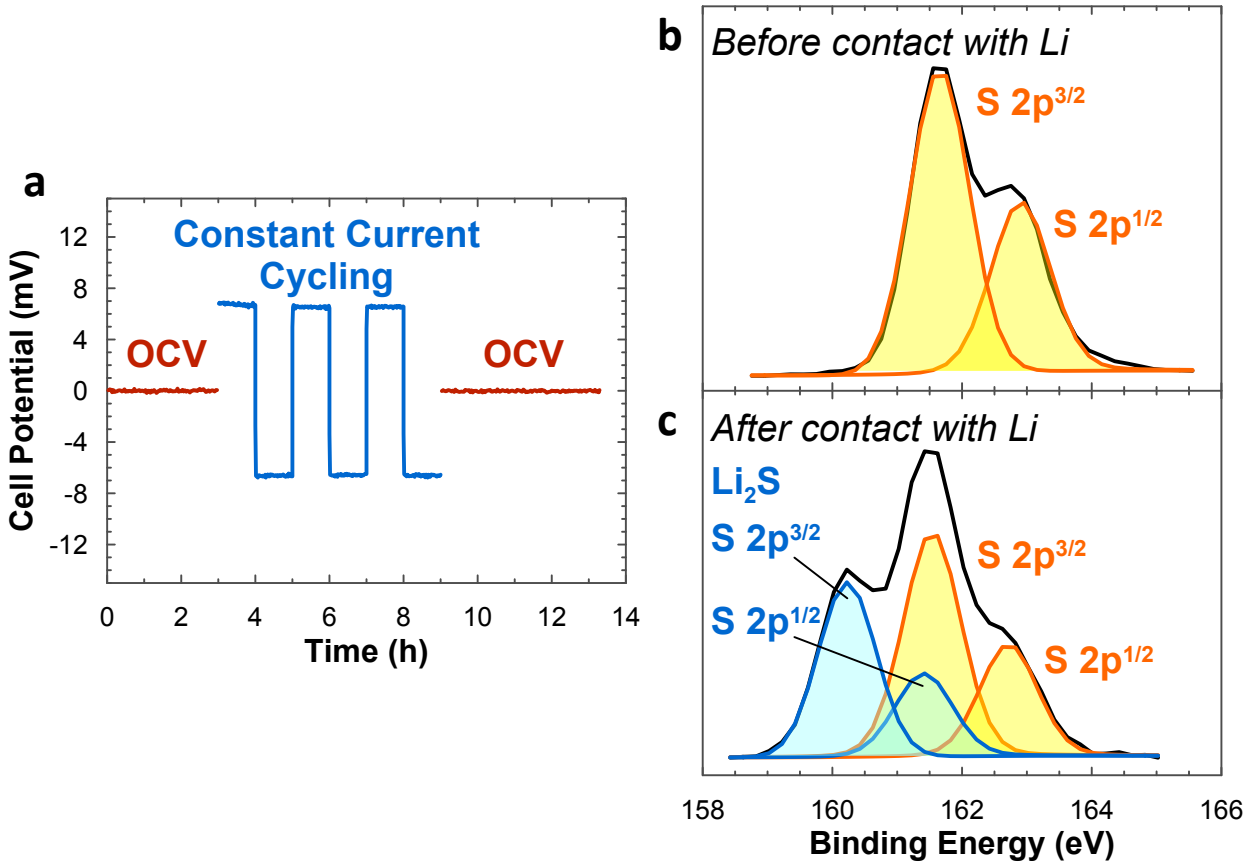

Figure S1: XPS of amorphous Li_3PS_4·½LiI pellets before and after being cycled 3 times in a Li/Li_3PS_4·½LiI/Li cell at 60°C and 0.2 mA/cm^2. a) The galvanostatic cycling procedure. b) Sulfur 2p XPS spectrum of a Li_3PS_4·½LiI pellet that has not been in contact with Li metal. c) Sulfur 2p XPS spectrum of a Li_3PS_4·½LiI pellet after contact with Li metal and three cycles.

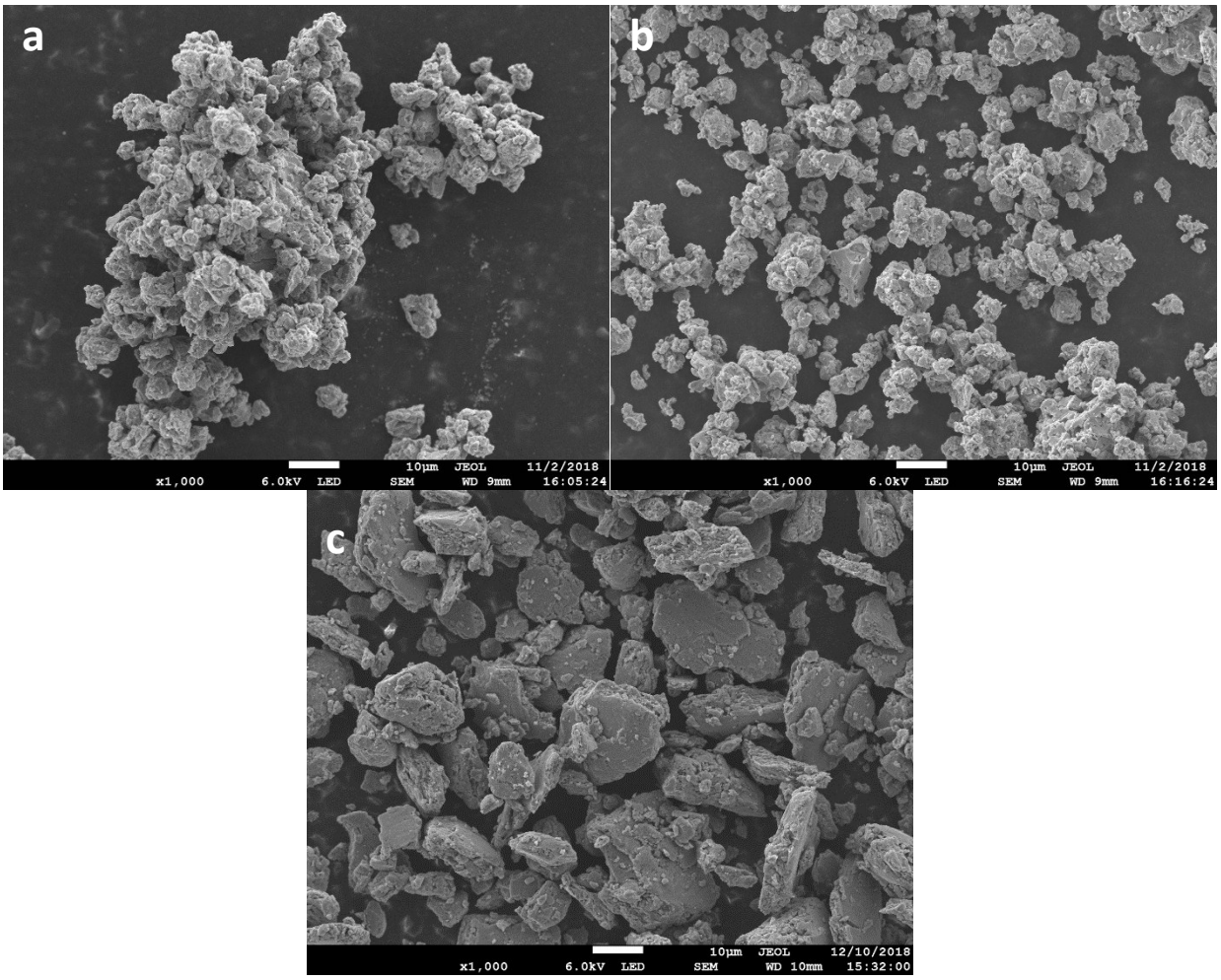

Figure S2: SEM images of (a) amorphous Li_3PS_4·½LiI, (b) nano-crystalline Li_3PS_4·½LiI after annealing the amorphous material at 185°C for 3 h, and (c) the sulfur-carbon-Li_3PS_4·½LiI composite after being ball-milled together. The white bar in all figures is 10 µm.

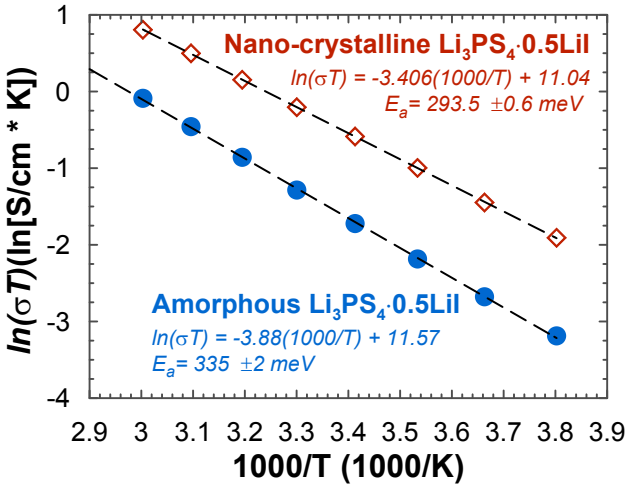

Figure S3: Arrhenius plot of the conductivities of both amorphous and nano-crystalline Li_3PS_4·½LiI.

The plot is used to calculate the Li^+ diffusion activation energy, E_a, from the equation $\sigma = \frac{\sigma_0}{T} e^{\frac{-E_a}{kT}}$.

The results were E_a(amorphous) = 335 ± 2 meV and E_a(nano-crystalline) = 293.5 ± 0.6 meV.

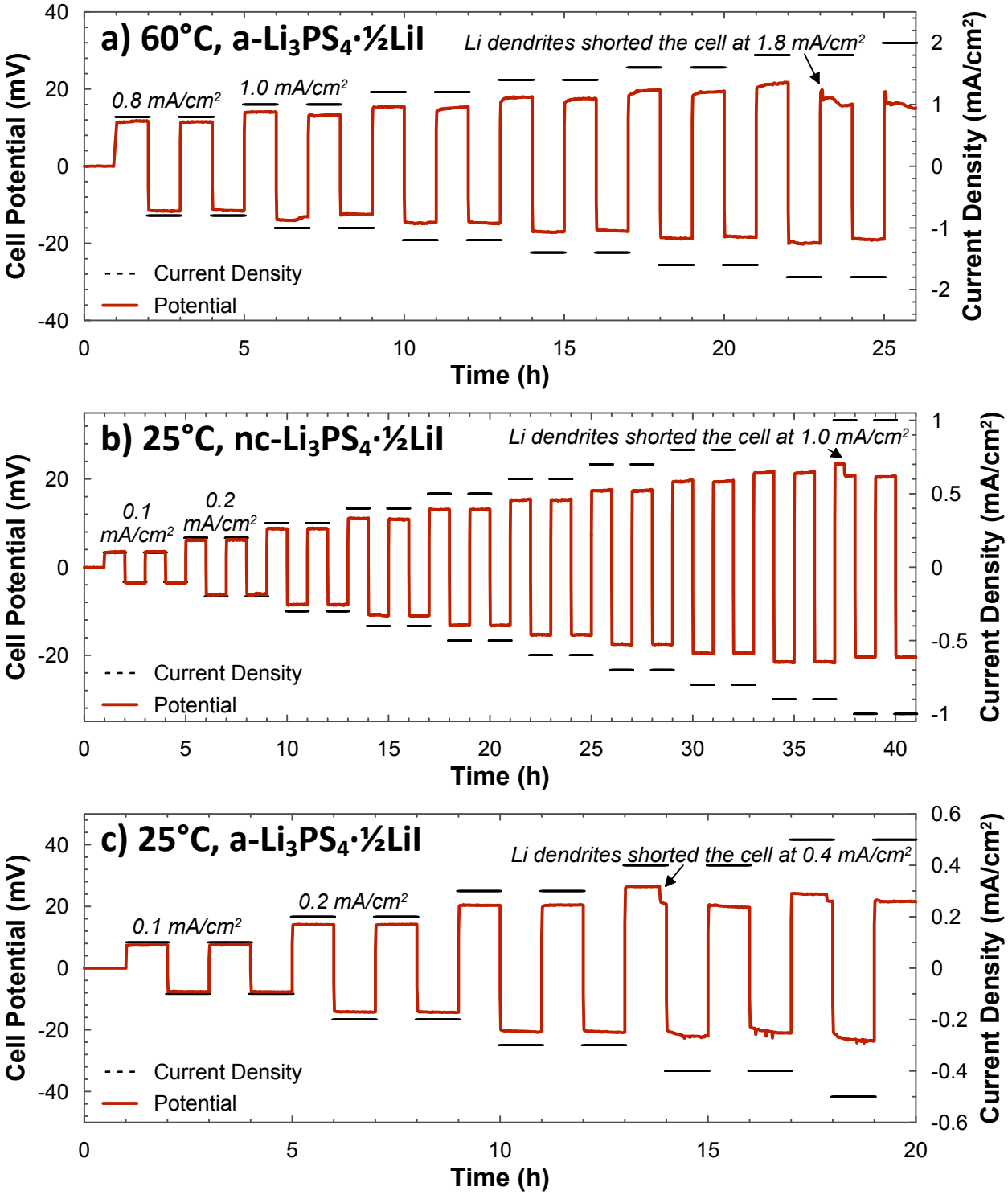

Figure S4: Critical current density tests of Li / Li_3PS_4·½LiI / Li cells. The current is held constant for two cycles, starting at 0.8 mA/cm², before rising in 0.2 mA/cm² steps to 4.0 mA/cm². a) Test performed with amorphous Li_3PS_4·½LiI at 60°C. b) Test performed with nano-crystalline Li_3PS_4·½LiI at 25°C. c) Test performed with amorphous Li_3PS_4·½LiI at 25°C.

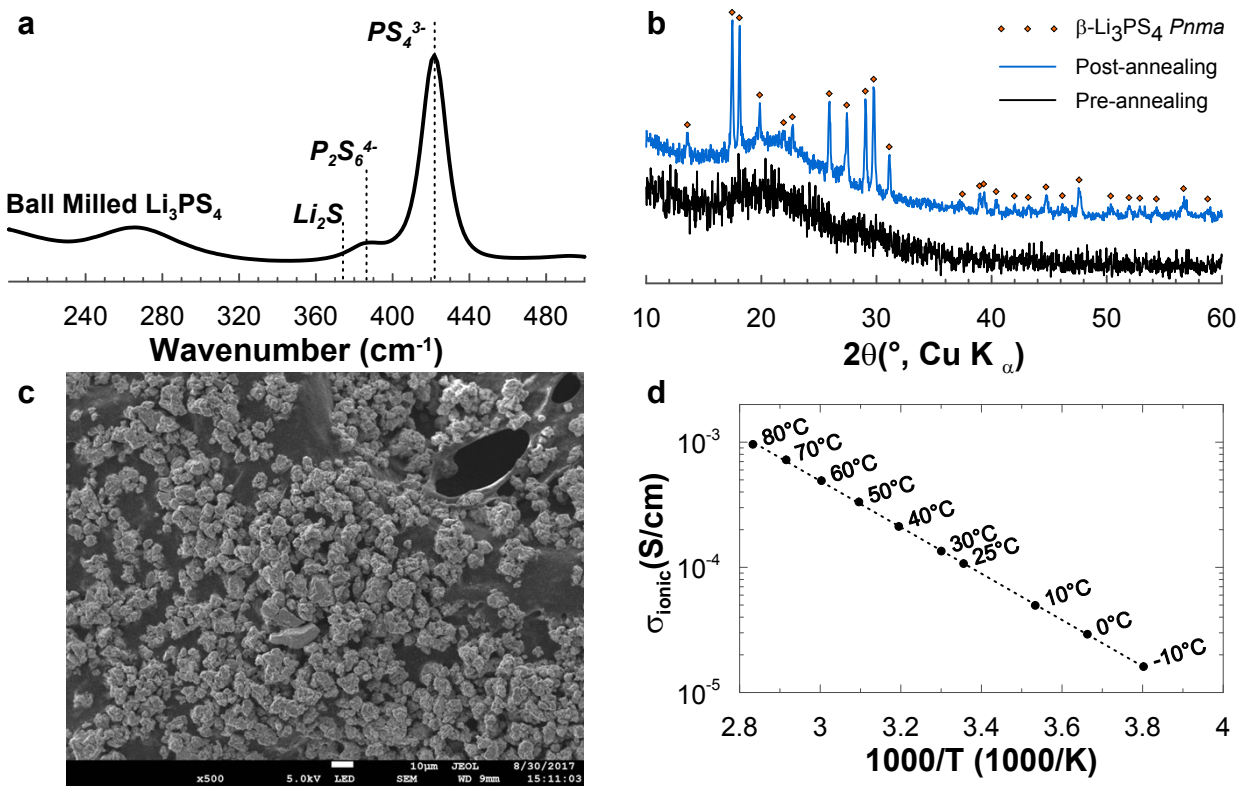

Figure S5: Characterization of ball-milled, amorphous Li_3PS_4 solid electrolyte. a) Raman spectroscopy showing primarily PS_4 tetrahedra with a small amount of P_2S_6 and no residual Li_2S. b) XRD patterns of Li_3PS_4 before (black) and after (blue) annealing. The absence of peaks before annealing indicates the initial powder is amorphous. c) SEM image of the amorphous Li_3PS_4 powder with an approximate particle size of 5 – 10 µm. d) The Arrhenius behavior of the Li^+-conductivity yields an activation energy of about 400 meV.

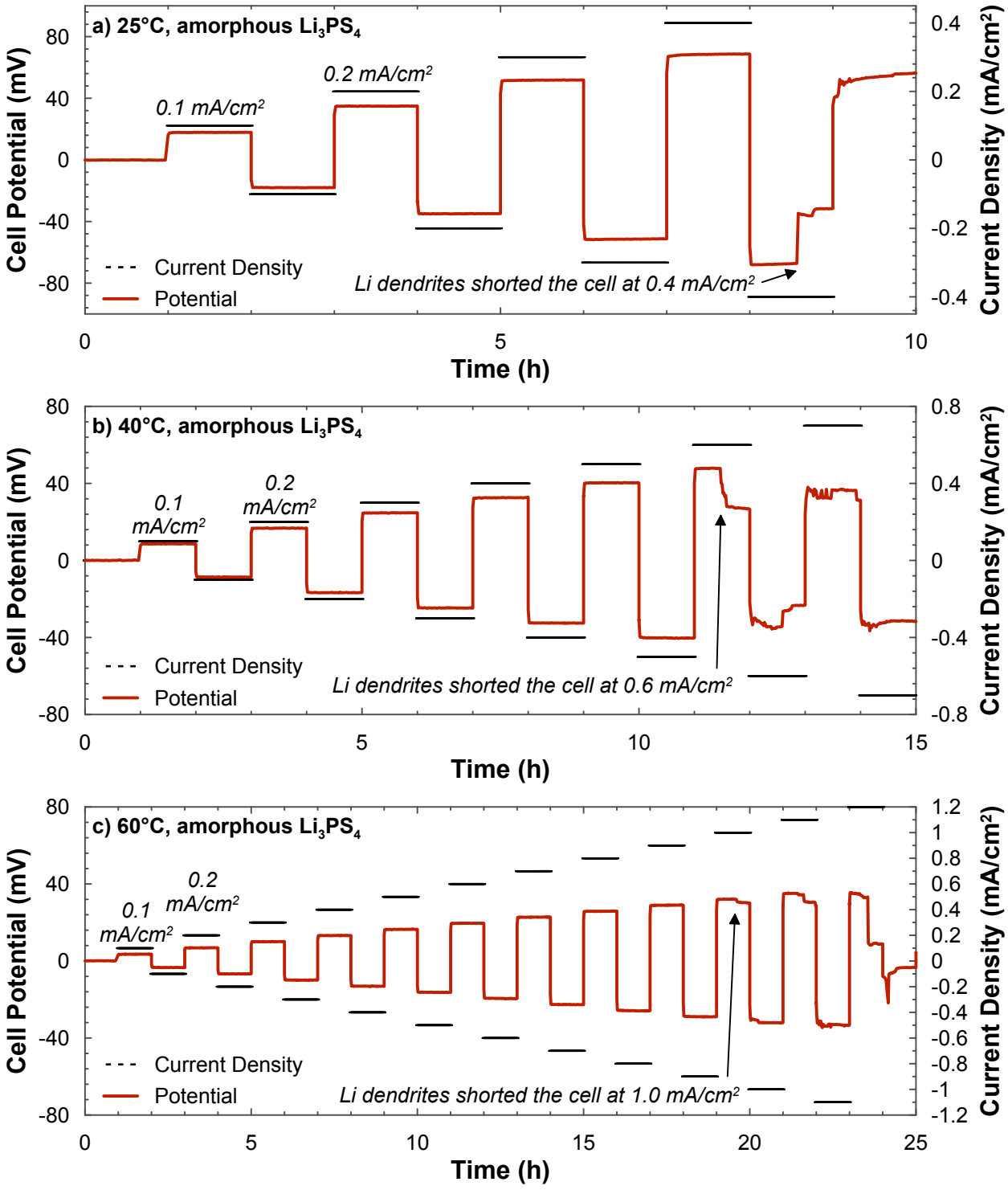

Figure S6: Critical current density of amorphous Li_3PS_4 at increasing Li^+-conductivities (i.e. temperatures): a) 25°C, b) 40°C, c) 60°C.

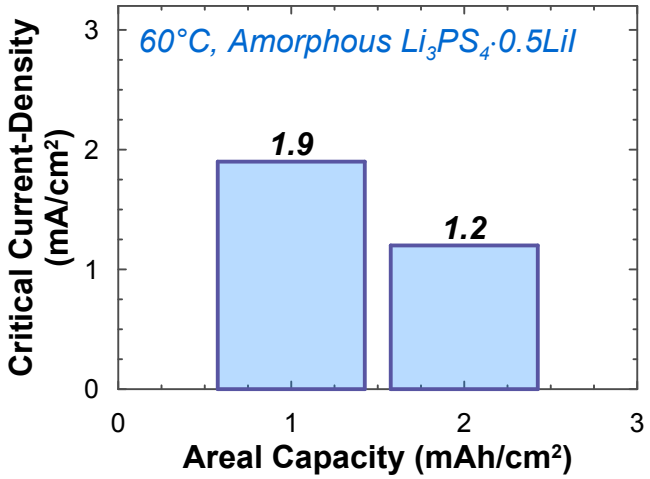

Figure S7: Critical current density as a function of the fixed areal capacity per half-cycle.

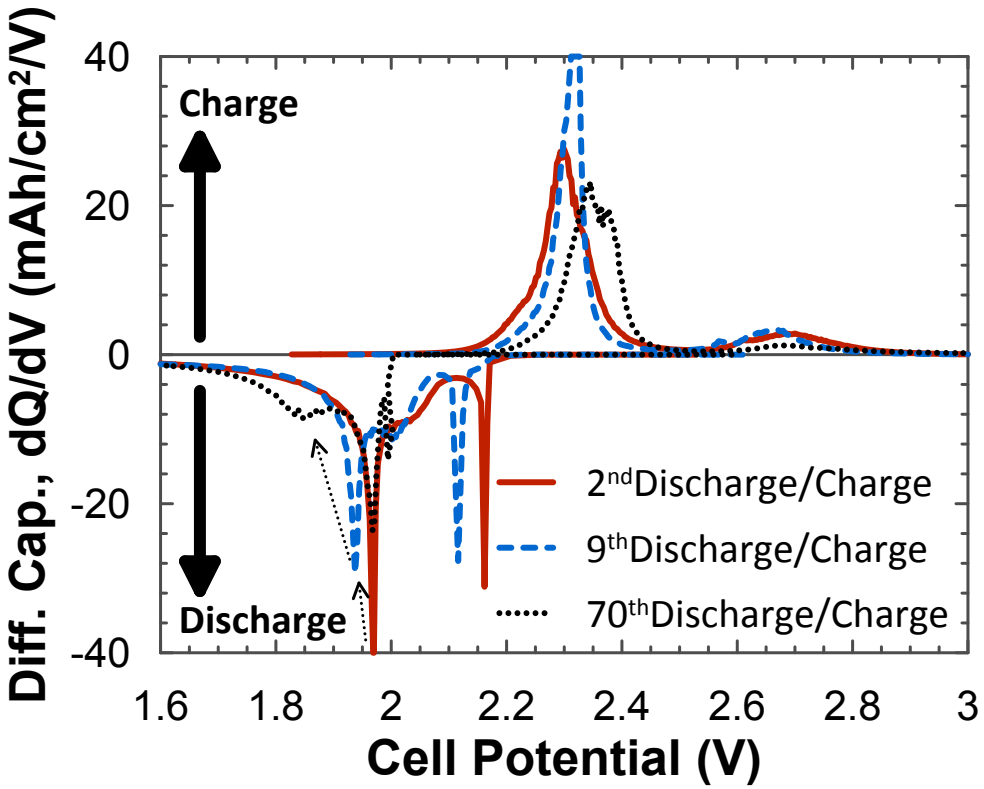

Figure S8: Differential capacity (dQ/dV) plot of cycles 2 (red), 9 (blue) and 70 (black) of a S-composite / nano-crystalline Li_3PS_4·½LiI / Li cell at 60°C. During discharge the peaks shift to lower potentials (shown by the dotted arrows) as cycling continues. Similarly, during charge the peaks shift to higher potentials. Both of these effects are likely due to an increase in cell impedance.

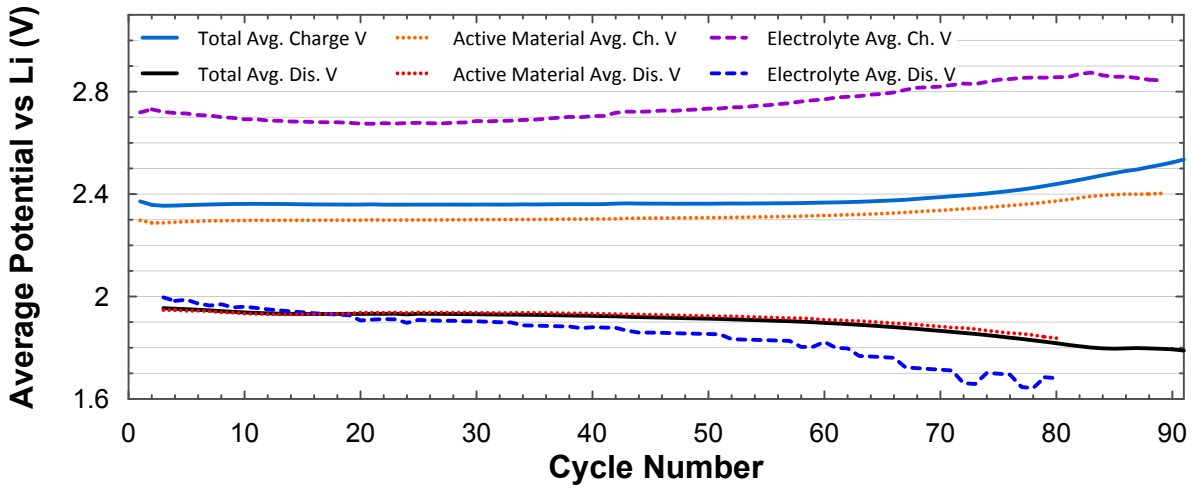

Figure S9: Average potential of the total charge (solid blue) or discharge (black) curves of a S-composite / nano-crystalline Li_3PS_4·½LiI / Li cell at 60°C as it is cycled. Additionally, the average potential of only the lower potential plateau (i.e. due to the S active material) during charge (orange) and discharge (red) is shown. Similarly, the average potential of only the upper potential plateau (i.e. due to the Li_3PS_4·½LiI solid electrolyte) during charge (violet) and discharge (dashed blue) is also shown.

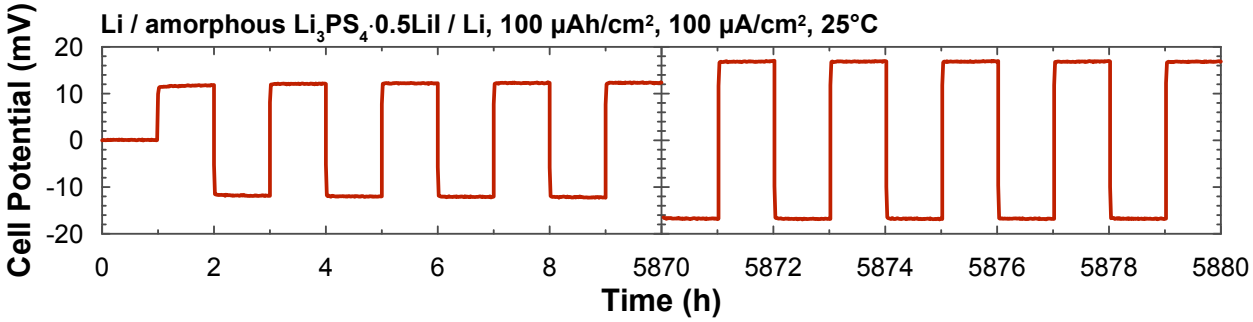

Figure S10: Galvanostatic cycling of a symmetric Li / amorphous Li_3PS_4·½LiI / Li cell at 25°C over more than 8 months. 100 μAh/cm² (~0.5 μm of Li) was cycled each half-cycle at 100 μA/cm².

Table S1: Data table showing the calculated changes in thickness of the sulfur electrode as it is reduced to Li_2S and the lithium electrode as it is consumed through oxidized. This calculation assumes 1,300 mAh/g S (i.e. utilization = 78%) is discharged in this hypothetical half-cycle and assumes zero porosity within the electrodes.

Sulfur			***Lithium***		
Mass =	2.12	mg/cm^2	**Mass =**	0.92	mg/cm^2
MM =	32.065	g/mol	**MM =**	6.941	g/mol
n =	6.62E-05	$moles/cm^2$	**n =**	1.32E-04	$moles/cm^2$
GCD =	1.672	mAh/mg	**GCD =**	3.861	mAh/mg
ACD =	3.548	mAh/cm^2	**ACD =**	3.548	mAh/cm^2
Density =	2	g/cm^3	**Density =**	0.534	g/cm^3
Thickness =	10.61	µm	**Thickness =**	17.21	µm
Li_2S					
Mass =	3.04	mg			
MM =	45.95	g/mol			
n =	6.62E-05	moles			
GCD =	1.167	mAh/mg			
ACD =	3.548	mAh/cm^2			
Density =	1.66	g/cm^3			
Thickness =	18.32	µm			
Volume change =	173%				
Positive thickness INCREASE during discharge:			7.71	µm	
Negative thickness DECREASE during discharge:			-17.21	µm	
Total thickness change during discharge:			-9.50	µm	

Reference

1 K. Minami, F. Mizuno, A. Hayashi and M. Tatsumisago, *Solid State Ion.*, 2007, **178**, 837–841.